Sci. Technol. Adv. Mater. **13** (2012) 035004 (6pp) doi:10.1088/1468-6996/13/3/035004

Direct stamping of silver nanoparticles toward residue-free thick electrode

Jiseok Kim[1], Kevin Wubs[1], Byeong-Soo Bae[2] and Woo Soo Kim[1]

[1] Mechatronic Systems Engineering, School of Engineering Science, Simon Fraser University, Surrey, BC V3T 0A3, Canada
[2] Department of Materials Science and Engineering, Korea Advanced Institute of Science and Technology, Daejeon 305-701, Republic of Korea

E-mail: woosook@sfu.ca

Received 3 February 2012
Accepted for publication 26 April 2012
Published 13 June 2012
Online at stacks.iop.org/STAM/13/035004

Abstract
Direct stamping of functional materials has been developed for cost-effective and process-effective manufacturing of nano/micro patterns. However, there remain several challenging issues like the perfect removal of the residual layer and realization of high aspect ratio. We have demonstrated facile fabrication of flexible strain sensors that have microscale thick interdigitated capacitors with no residual layer by a simple direct stamping with silver nanoparticles (AgNPs). Polyurethane (PU) prepolymer was utilized as an adhesive layer to transfer AgNPs more efficiently during the separation step of the flexible stamp from directly stamped AgNPs. Scanning electron microscopy images and energy dispersive x-ray spectroscopy analysis revealed residue-free transfer of microscale thick interdigitated electrodes onto two different flexible substrates (elastomeric and brittle) for the application to highly sensitive strain sensors.

Keywords: direct stamping, silver nanoparticles, flexible sensors, strain sensors

1. Introduction

Patterning of conductive media directly on a substrate has attracted much interest to overcome restrictions of indirect patterning techniques [1–9]. Patterning of metal on electronic devices is required for creating a conducting pass between active components or electrodes to apply potential and to receive signals [10]. Importantly, the patterning methods should leave no conductive residual layer between conductive patterns to avoid a short circuit. At first, indirect patterning methods were introduced to achieve this requirement [11–15]. Researchers have successfully made patterned conductors on conventional substrates such as silicon by microtransfer stamping [14] or photolithography [15] combined with metal evaporation and metal lift-off process. However, these processes require special equipment and environment such as vacuum, chemical etching, and high temperature and pressure. Thus, patterning of conductive media needs highly process-efficient and cost-efficient fabrication methods. In addition, recently, mechanically ductile substrates such as polymers have been drawing much attention as demand for flexible and cheap electronic devices have increased in many areas [16]. Flexible substrates usually do not tolerate the harsh environment associated with the above-mentioned patterning methods. Thus, variants of direct patterning methods have been developed to overcome the limitations. Some important techniques include nanotransfer printing (nTP) [1–3, 7], direct imprinting [4, 5], liquid-bridge transfer stamping (LB-nTM) [8], laser direct curing (LDC) [9] and direct ink writing [6].

Among these techniques, direct imprinting of silver nanoparticles [4], water-mediated nTP [7] and LB-nTM [8] have been reported as simple and cost-effective methods. These methods are variants of soft lithography using inexpensive elastomeric materials for pattern transfer. Polydimethylsiloxane (PDMS) is the most common elastomeric material owing to its excellent properties such as a low surface energy. Aforementioned direct patterning of functional materials demonstrated successful formation of structures, but they still have limitations. For the direct imprinting, relatively high stamping temperature and pressure are still required to fill functional materials into stamp well

and, importantly, to minimize the amount of residue layer. LB-nTM needs a specific substrate having a high surface free energy to achieve capillary action strong enough to detach stamped materials from a stamp. For nTP, metal should be evaporated in vacuum, thermally or by electron-beam, either on a stamp or an ink pad, and the stamp or the ink pad also needs surface treatment with anti-adhesive materials to ensure clear detachment of metal. All these restrictions may add complexity and cost to the techniques. Besides, the ability of these methods to transfer microscale metal patterns with a high aspect ratio seems to be limited. Higher temperature and pressure should be required for direct imprinting to minimize the residual layer and to fill a stamp. Also for LB-nTM, effective capillary force cannot be available for microscale patterns with a high aspect ratio.

In this study, we introduce UV-curable adhesive-mediated direct stamping of metal nanoparticles. For the main idea of this novel method, UV-curable PU prepolymer was used as an adhesive layer to efficiently transfer silver nanoparticles (AgNPs) pattern onto the target substrate. This direct stamping method has been applied to fabricate a strain sensor made of micron-thick interdigitated electrodes without any residual layer. Durability is required from a strain sensor, such as one for the intelligent tire sensors, exposed to harsh environment like repeatable, irregular and abrupt deformation. A flexible tire sensor fabricated by photolithography with metal lift-off had a very thin film of electrodes [17], which might not be strong enough to endure harsh exploitation conditions. Hence, the thick electrodes fabricated in this work by the direct stamping of metal nano ink might help enhance the durability of the sensor.

2. Experimental details

2.1. Materials

PDMS elastomer (Sylgard 184) and cross-linker were obtained from Dow Corning. Silver paint was purchased from SPI supplies. Silver acetate, hexadecylamine, phenylhydrazine, toluene, acetone, methanol and polyethylene glycol monomethyl ether acetate (PGMEA) were purchased from Sigma-Aldrich for the synthesis of AgNPs. Urethane acrylate (EBECRYL 265 photo-curable resin) and photo-initiator (Irgacure 184) were obtained from Cytec Industries and CIBA, respectively. All the reagents were used as received.

2.2. Synthesis of silver nanoparticles

AgNPs were synthesized with modification from the method reported in [18]. In brief, hexadecylamine was dissolved in toluene at 60 °C. Silver acetate was added and dissolved into the solution at 60 °C. Then, phenylhydrazine was mixed into toluene and added dropwise to the solution including hexadecylamine and silver acetate. The mixture was stirred for 1 h, precipitated into acetone/methanol (100 ml/100 ml). The precipitated silver nanoparticles were dried at ambient temperature for 24 h. Then, the silver nanoparticles were dispersed in chloroform for further use as ink. AgNPs annealed at 150 °C for 30 min showed a high conductivity of (2.0–4.0) $\times 10^4$ S cm^{-1}.

2.3. UV curable adhesive-mediated direct stamping of silver nanoparticles

A flexible PDMS stamp was replicated from a silicon master patterned by the conventional photolithography. Figure 1(a) shows the main steps of UV-curable adhesive-mediated direct stamping. Firstly, the AgNP ink [18] (40 wt% AgNPs in chloroform, viscosity about 25 cP) was filled in the trenches of the flexible PDMS stamp and excess of the AgNP ink was removed with a piece of flexible polyethylene terephthalate (PET) film. Then, an adhesive film was placed on the PDMS stamp to remove the residual layer on the protruded surface, and the AgNP ink in the PDMS stamp was left to dry for 5 min at ambient temperature, ∼23 °C. Then, the PDMS stamp was brought onto the substrate, which was spread with 0.1 ml of UV-curable PU prepolymer (urethane acrylate 90 wt% and photo-initiator 5 wt% in PGMEA, middle of figure 1(a)). PDMS and glass-fabric reinforced hybrimer (GFR-hybrimer) were used as the flexible substrates. The whole stamp with the UV-curable PU prepolymer on each substrate was exposed for 10 min to UV light (365 nm, 3 mW cm^{-2}) from a Black-Ray B-100AP high-intensity UV lamp. Afterwards, the PDMS stamp was peeled off to leave a pattern of AgNPs on the substrate. For the final step, the pattern of AgNPs transferred on the substrate was annealed at 150 °C for 30 min to convert it into highly conductive silver.

2.4. Fabrication of a strain sensor by direct stamping

A flexible strain sensor with interdigitated micron-thick electrodes was fabricated to confirm the applicability of direct stamping method in intelligent tire sensors. The fabricated strain sensor was observed in a Strata DB235 field emission scanning electron microscope (FESEM) after coating of gold on the sample. Elemental analysis of the strain sensor was carried out using an energy dispersive x-ray spectroscopy (EDS) instrument attached to the FESEM.

2.5. Characterization of the strain sensor

Strain sensors were prepared on two substrates differing in mechanical properties — brittle (GFR-hybrimer [19]) and elastomeric (PDMS). The initial capacitance for a strain sensor was measured as ∼3 pF, which is reasonably high. Each sensor was installed in a GUNT WP300 universal material tester, and capacitance was measured *in situ* using an Agilent E4980 precision LCR meter at 1 MHz as the sensor was stretched out axially. Capacitance was registered every 10 μm of length change in the sensor. For the bending test, capacitance was registered using the LCR meter at 1 MHz as the strain sensor was placed on cylinders having different radii between 2.5 and 38.5 mm.

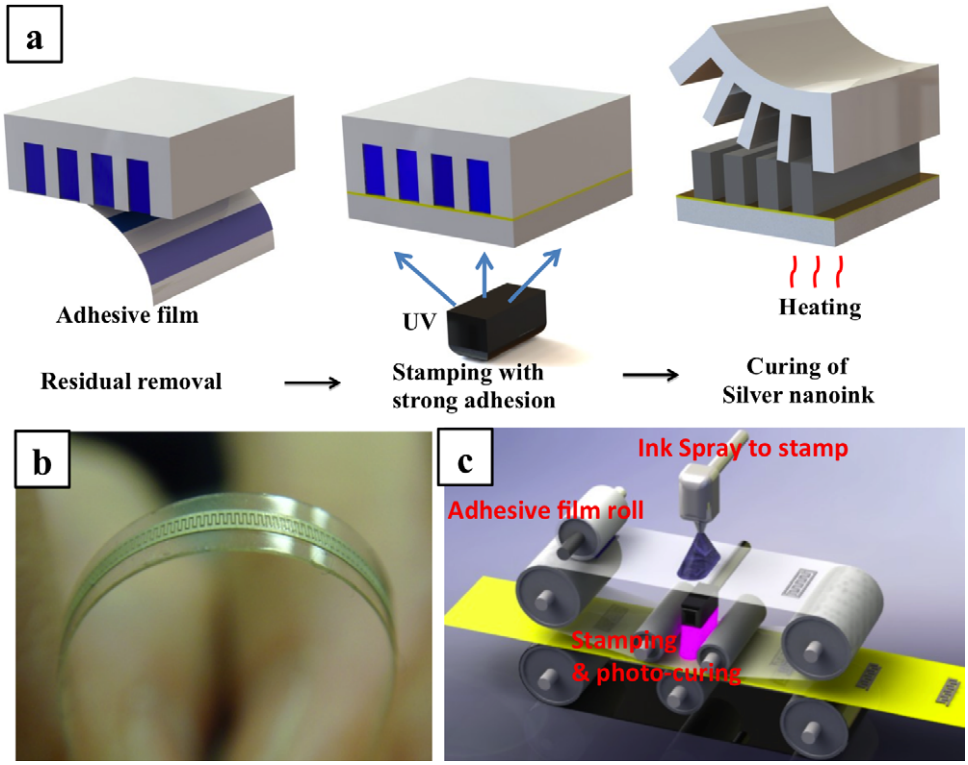

Figure 1. (a) Schematic of the three main steps of the direct stamping: (i) removal of AgNP residual layer (blue stripes) by an adhesive film after filling the stamp with AgNPs, (ii) UV-curing after the PDMS stamp is brought onto a substrate spread with PU prepolymer (yellow layer) and (iii) thermal curing of AgNPs after separation of the PDMS stamp. (b) Image of a sample patterned by the direct stamping method. (c) A roll-to-roll instrument designed to apply the direct stamping method to fabrication of electronic devices. Fabrication processes are continuously performed for the final product by rolls. An adhesive roll removes the residual layer after ink-spraying on a stamp, pattern is transferred on the substrate coated with a photo-curable PU layer (yellow), and then UV and heat-curing follow to finalize the product.

3. Results and discussion

Our direct stamping basically includes filling of AgNP ink into the trenches of the stamp, removal of the residual layer on protrusion surfaces of the stamp, transferring the AgNP pattern on a substrate and annealing AgNPs. Figure 1(a) illustrates main processes from removal of the residual layer to annealing of AgNPs. When AgNP ink was doctored off on the PDMS stamp, AgNPs filled the trenches of the stamp and also remained on unwanted surfaces of the stamp between patterns. This unwanted residual layer of AgNPs can be perfectly removed by an adhesive film. The blue stripes on the adhesive film in figure 1(a) schematically represent the unwanted residual layer of AgNPs attached from the protruded surfaces of the stamp. Only the unwanted AgNPs were easily attached on the adhesive film while the pattern of AgNPs inside the trenches of the stamp was left intact. This is because PDMS material itself has an anti-sticking property owing to its low surface energy and because the decrease in volume of AgNPs after drying leaves an empty room between the adhesive film and the AgNPs in the trenches of the stamp. The small empty room might prevent the adhesive film from sticking to the AgNPs inside the trenches.

Next, the UV-curable PU was used as an adhesive layer to enhance the transfer of the AgNPs onto a flexible substrate. The yellow layer in figure 1(a) describes the PU film spread between the PDMS stamp and the substrate. No additional pressure was applied when the PDMS stamp was placed on the substrate because the weight of the PDMS stamp itself was enough to make conformal contact between the PU prepolymer on the substrate and the AgNPs inside the stamp. The high viscosity of PU helped it to fill the small empty room above the AgNPs in the stamp and thus the conformal contact with the substrate could be enhanced without any additional pressure or heat. In a microscopic view, adhesion becomes an important interaction for the contact between two objects. Provided there is no special interaction when two solids contact each other, adhesion is dependent on the surface free energy and the real contact area between two solids [20]. Clean transfer of AgNPs from a stamp onto the substrate might be possible if adhesion between AgNPs and the substrate is sufficiently higher than that between AgNPs and the PDMS stamp. When a hard sphere of AgNP and a flat elastic surface make contact, the surface deforms due to van der Waals force between them. The real contact area is determined by this deformation. Van der Waals force can be calculated using equation (1) [21] and is high enough to deform the PDMS stamp even by one AgNP particle owing to the low elastic modulus of PDMS.

$$F_{\mathrm{vdw}} = 3.2 \times 10^{-15} \frac{hd}{z_0^2} + 6.4 \times 10^{-15} \frac{ha_0^2}{z_0^3} [N] \qquad (1)$$

Here, h is the van der Waals constant in eV, d is the particle diameter in μm, z_0 is the adhesion distance in Å and a_0 is the

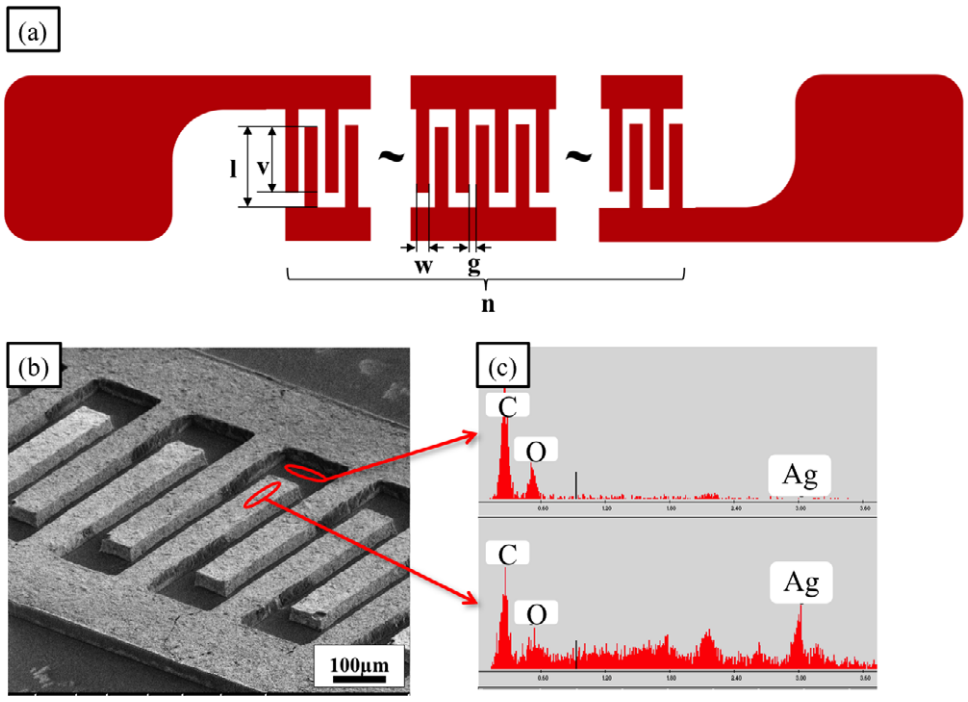

Figure 2. (a) Design of an interdigitated strain sensor, l: length of each interdigitated finger electrode, v: overlapping length between two adjacent electrodes, w: width of each electrode, g: gap between two adjacent electrodes, n: total number of electrodes. (b) SEM image of an interdigitated strain sensor fabricated by the direct stamping, (c) EDS analysis of one electrode and a gap between electrodes.

radius of the adhesive contact area in μm induced by the first force term. The first term is the van der Waals force caused before any contact, and the second term is the additional van der Waals force caused by deformation induced by the first term.

This high van der Waals force might enable the PDMS stamp to maximally contact one AgNP by about a half surface area of it. However, the full contact becomes impossible for a AgNP aggregate because the elastic restoring force of PDMS due to intramolecular bonds does not allow PDMS to flow and fill the gaps between the AgNPs. Thus, the real contact area between PDMS and AgNPs remains much smaller than the sum of the contact areas of individual AgNPs. On the other hand, viscous UV-curable PU prepolymer can easily flow and fill the gaps between AgNPs to make full contact between the PU prepolymer layer and AgNPs. Afterwards, the PU prepolymer layer is UV-cured into a PU film and the real contact area between them remains maximal. Surface free energies of PU ($\sim$25 mJ m^{-2}) and PDMS ($\sim$20 mJ m^{-2}) are similar, but the PU adhesion layer has much larger real contact area than the PDMS stamp does, which leads to a significant difference in adhesion force. As a result, the adhesion between the UV-cured PU layer and AgNPs becomes much stronger than that between the PDMS stamp and AgNPs, and thus clean transfer of AgNPs inside the PDMS stamp onto the substrate can be realized with the PU adhesive layer. Without the PU layer, AgNPs should directly contact the substrate, and then AgNPs might fail to make full contact with the substrate hindering the clean transfer of AgNPs from the stamp. GFR-hybrimer is much harder than PDMS (Young's modulus is $\sim$10 GPa for GFR-hybrimer but $\sim$2 MPa for PDMS.), so van der Waals force does not deform the GFR-hybrimer as much as PDMS. Thus, for a GFR-hybrimer substrate, the real contact area and the adhesion force become much smaller, impeding the transfer of AgNPs onto the bare GFR-hybrimer substrate. Thus, the PU layer is very helpful for a clean transfer of AgNPs onto the GFR-hybrimer substrate.

Direct stamping benefits from the use of AgNPs ink because the small AgNPs can be homogeneously dispersed into a liquid form. Besides, the melting point of AgNPs can be as low as 150 °C [22] allowing formation of conductive material from AgNPs upon mild heating. Thus, the polymer substrates which have much lower melting point than bulk silver can survive the annealing of AgNPs. The final silver pattern on the substrate is shown in figure 1(b) as held by hand. All stamping steps are simple to be adapted for a roll-to-roll process combined with spraying of AgNP ink as suggested in figure 1(c). The roll-to-roll direct stamping method might contribute to high throughput and material efficiency for fabrication of micro- and nanoelectronic devices.

A strain sensor with interdigitated electrodes was chosen for application of the direct stamping technique to demonstrate the advantage of our direct stamping technique. The sensor design is shown in figure 2(a). The length (l) and width (w) of the finger electrode, the overlapping length (v) and gap (g) between two adjacent fingers and the thickness of the electrodes were 500, 80, 400, 40 and 40 μm, respectively. The total number of pairs of two adjacent fingers (n) was 200.

The working principle of the strain sensor is simple. Each pair of adjacent finger electrodes can be considered as a capacitor [23]. Deformation of the sensor changes the overlapping length and the distance between those two adjacent finger electrodes. As a result, the sensor's

capacitance varies [17]. For the strain sensor to work properly, it is very important to remove the residual layer of AgNPs between the finger electrodes because a contact between any pair of adjacent fingers will short-circuit the whole device. The SEM image in figure 2(b) clearly shows the absence of silver residue between the interdigitated finger electrodes, which was also confirmed by EDS analysis (figure 2(c)). The thick layer of AgNPs was successfully transferred onto the substrate maintaining almost the same shape of the sensor designed on the silicon master. Originally designed dimensions (figure 2(a); $l = 500$, $v = 400$, $w = 80$, $g = 40$, $t = 40\,\mu$m) were reduced by about 10% ($l_{ss} = 450$, $v_{ss} = 350$, $w_{ss} = 70$, $g_{ss} = 35$, $t_{ss} = 35\,\mu$m where l_{ss} is length of each finger electrode of the stamped strain sensor, v_{ss} overlapping length between two adjacent electrodes, w_{ss} width of each finger electrode, g_{ss} gap between two adjacent electrodes and t_{ss} thickness of each electrode). This small reduction should be caused by the decrease of the volume of AgNPs after thermal curing, during which surfactant molecules surrounding AgNPs are burned away and AgNPs are sintered to fuse together. In addition, the thickness of the PU layer was measured as $\sim 7\,\mu$m and the thickness of the interdigitated electrode made of AgNPs above the PU layer was about 28 μm. These results confirmed the fabrication of thick silver electrodes.

The interdigitated strain sensor was designed to obtain a high capacitance within a small area and a uniform distribution of strain over the capacitor area when the sensor is under tensile stress. Stress was uniformly distributed over the sensor as shown by the tensile simulation of figure 3(a) when the sensor was stretched out at both ends.

Capacitance decreased under the tensile stress as the overlapping length of two adjacent finger electrodes was reduced and the gap between the adjacent finger electrodes increased. The reduction of the overlapping length is caused by the Poisson effect which describes the change in length perpendicular to an applied load. This Poisson effect accounts for the substrate dependency of the sensor because the Poisson's ratio is different from material to material. The direct stamping allowed for successful fabrication of the strain sensors on the two different substrates, PDMS and GFR-hybrimer. PDMS is hydrophobic and stretchable while GFR-hybrimer is hydrophilic and brittle. As expected from the working principle of the interdigitated strain sensor, capacitance was decreased according to elongation of the sensor on the tensile tester. Relative capacitance changes were calculated from the registered capacitance changes divided by the initial capacitance of the sensor to make comparison of the two substrates reliable. Tensile test of the stamped strain sensors could be easily performed on a conventional tensile tester. The installation of the sensor is shown in figure 3(b) and the results are plotted in figure 3(c). Gauge factors (GFs) which represent the sensitivity of a strain sensor to strain were obtained from the slopes of the graphs of figure 3(c) as -3.07 and -0.391 for PDMS and GFR-hybrimer, respectively. The GF was much larger for the strain sensor on PDMS than on GFR-hybrimer because the brittle GFR-hybrimer has a low Poisson's ratio of ~ 0.1. Although change in the distance

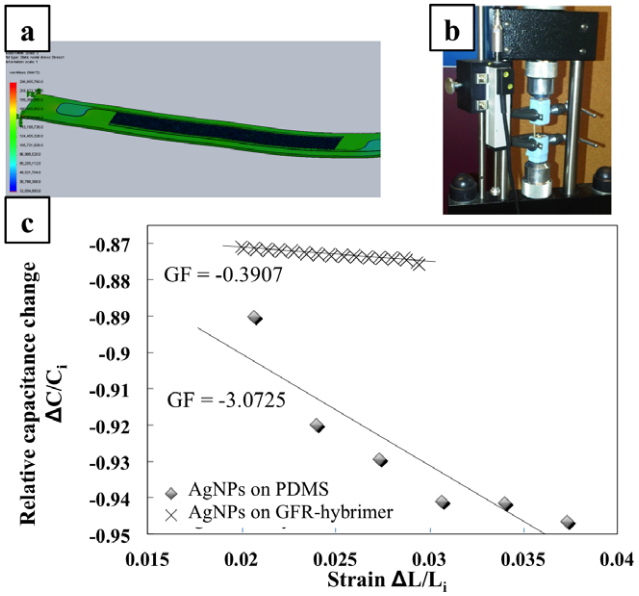

Figure 3. (a) Tensile-simulated deformation result which shows uniform distribution of stress over the strain sensor. For tensile stress, the left end is fixed and ~ 1 mN of tensile load is applied to the right end. (b) Conventional tensile tester with the strain sensor sample loaded. (c) Relative capacitance versus tensile strain for flexible strain sensors fabricated on PDMS and GFR-hybrimer substrates.

between the adjacent finger electrodes was the same for both substrates because the change was in the same direction as the tensile strain, the reduction of overlapping length between the electrodes varied because the Poisson's ratio was different in each substrate. Also, the number of pairs of interdigitated finger electrodes benefited the GF of the strain sensor due to the Poisson effect. For example, the total change of overlapping length between adjacent electrodes increases two times when the number of electrode pairs doubles – thus, the more the adjacent electrode pairs, the larger the change of capacitance. This might help to reliably detect small strain. A strain sensor does not work reliably if an absolute capacitance change is not large enough to be registered as compared to noise, even though the relative capacitance changes according to strain are the same in two different strain sensors. Thus, the UV-curable adhesive-mediated direct stamping method has enabled us to fabricate many more pairs of interdigitated electrodes in a small length. Accordingly, a reliable, sensitive, small and cost-effective strain sensor could be fabricated.

Bending test has been also performed to see how the stamped strain sensor works when it bends, as bending should be another mode for a strain sensor. Bending simulation in figure 4(a) shows uniform distribution of stress over the region where the strain sensor bends.

The strain sensor was put around a cylinder as shown in figure 4(b) and capacitance was measured as the radius of the cylinder was decreased. As shown in figure 4(c), capacitance remains almost constant down to a certain radius of curvature (~ 10 mm) at which the capacitance starts to decrease due to the increase of the gap between adjacent fingers. The initial distance between two adjacent fingers is

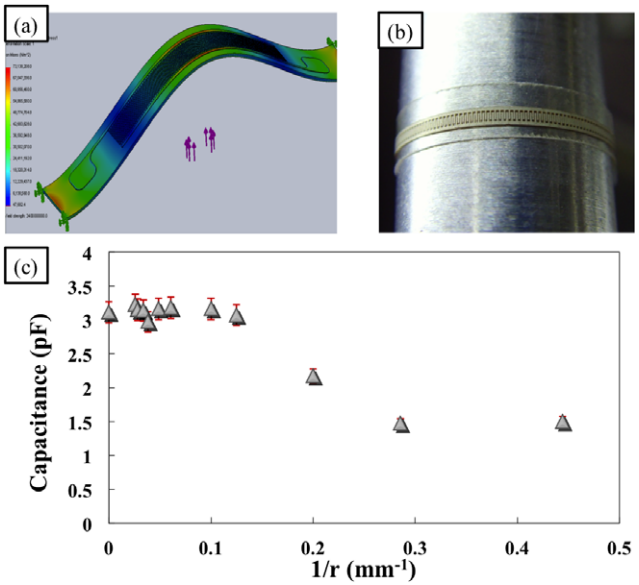

Figure 4. (a) Bending-simulated deformation result which shows uniform distribution of stress over the area where the strain sensor bends. Both ends are fixed and ∼1 mN is applied in the middle of the sensor from below. (b) Image of the flexible strain sensor wrapping around a cylinder for measurement of change in capacitance according to curvature. (c) Change in capacitance of the flexible strain sensor with curvature.

35 μm (from the SEM image) which is much smaller than the radius of curvature under the bending test. So, at the relatively large radii (>10 mm), the gap between the adjacent fingers remains relatively small, and the change in capacitance is not large enough to be registered. When the radius of curvature becomes even smaller, the sensor capacitance starts to decrease. As capacitance is inversely proportional to the gap, change in capacitance is high at first and then decreases as shown in the graph.

4. Conclusions

We have successfully fabricated thick conductive patterns directly on flexible substrates by the direct stamping of AgNPs. The adhesive PU layer allowed clean and easy transfer onto flexible substrates with perfect contact of AgNPs to the inside trenches of the stamp. The PU adhesive layer was viscous enough to contact fully the surface of all AgNPs, so that PU layer provides much higher adhesion force with AgNPs than the bare PDMS stamp does. The difference in adhesion force enables easy transfer of AgNPs from the stamp onto a substrate. Applicability of this direct stamping technique has been confirmed by fabrication of highly sensitive and cost-effective strain sensors on flexible substrates like PDMS and GFR-hybrimer for the intelligent tire sensor. The directly stamped strain sensor has properly responded to strain under both tensile and bending stresses. Thus, the reported direct stamping overcomes restrictions of other direct metal patterning methods and opens a way to direct patterning of a metal on a flexible substrate in ambient environment without any complex processes. Furthermore, a continuous roll-to-roll process is expected to be easily applicable to the direct stamping for high-throughput fabrication of electronic devices.

Acknowledgments

This work received financial support from the Discovery Grant Program funded by the Natural Sciences and Engineering Research Council of Canada (NSERC) as well as the Auto 21 Project Grant Program (F504-FTS).

References

[1] Loo Y L, Willett R L, Baldwin K W and Rogers J A 2002 *J. Am. Chem. Soc.* **124** 7654
[2] Loo Y L, Lang D V, Rogers J A and Hsu J W P 2003 *Nano Lett.* **3** 913
[3] Lee B H, Cho Y H, Lee H, Lee K-D, Kim S H and Sung M M 2007 *Adv. Mater.* **19** 1714
[4] Ko S H, Park I, Pan H, Grigoropoulos C P, Pisano A P, Luscombe C K and Frechet J M J 2007 *Nano Lett.* **7** 1869
[5] Park I, Ko S H, Pan H, Grigoropoulos C P, Pisano A P, Frechet J M J, Lee E-S and Jeong J-H 2008 *Adv. Mater.* **20** 489
[6] Ahn B Y, Duoss E B, Motala M J, Guo X Y, Park S I, Xiong Y J, Yoon J, Nuzzo R G, Rogers J A and Lewis J A 2009 *Science* **323** 1590
[7] Oh K, Lee B H, Hwang J K, Lee H, Lee K H, Im S and Sung M M 2009 *Small* **5** 558
[8] Hwang J K, Cho S, Dang J M, Kwak E B, Song K, Moon J and Sung M M 2010 *Nature Nanotechnol.* **5** 742
[9] Kang B, Ko S, Kim J and Yang M 2011 *Opt. Express* **19** 2573
[10] Julia W P H 2005 *Mater. Today* **8** 42
[11] Bailey R C, Stevenson K J and Hupp J T 2000 *Adv. Mater.* **12** 1930
[12] Kumar A and Whitesides G M 1993 *Appl. Phys. Lett.* **63** 2002
[13] Li X G, Tian Y, Xia P P, Luo Y P and Rui Q 2009 *Anal. Chem.* **81** 8249
[14] Stevenson K J, Hurtt G J and Hupp J T 1999 *Electrochem. Solid St.* **2** 175
[15] Knight M W, Sobhani H, Nordlander P and Halas N J 2011 *Science* **332** 702
[16] Gundlach D J 2007 *Nature Mater.* **6** 173
[17] Matsuzaki R, Keating T, Todoroki A and Hiraoka N 2008 *Sensors Actuators a—Phys.* **148** 1
[18] Li Y N, Wu Y L and Ong B S 2005 *J. Am. Chem. Soc.* **127** 3266
[19] Jin J H, Ko J H, Yang S and Bae B S 2010 *Adv. Mater.* **22** 4510
[20] Joo S C and Baldwin D F 2010 *Nanotechnology* **21** 055204
[21] Bowling R A 1985 *J. Electrochem. Soc.* **132** 2208
[22] Greer J R and Street R A 2007 *Acta Mater.* **55** 6345
[23] Kidner N J, Homrighaus Z J, Mason T O and Garboczi E J 2006 *Thin Solid Films* **496** 539